High pressure SANS studies of glucose isomerase conformation in solution

Ewa Banachowicz,[a] Maciej Kozak,[a*] Adam Patkowski,[a] Gerhard Meier[b] and Joachim Kohlbrecher[c]

[a]Institute of Physics, A. Mickiewicz University, Umultowska 85, 61-614 Poznan, Poland, [b]Forschungszentrum Juelich Institute of Solid State Research Postfach 1913, 52428 Juelich, Germany, and [c]Laboratory for Neutron Scattering, ETH Zurich & Paul Scherrer Institut, CH-5232 Villigen PSI, Switzerland.

E-mail: mkozak@amu.edu.pl

Synopsis Small-angle neutron scattering (SANS) studies of glucose/xylose isomerase indicate that the structure of this protein in solution is very stable and very similar to that in a crystal, in a broad pressure range up to 150 MPa. This enzyme can be used as a secondary standard for SANS measurements.

Abstract Small-angle neutron scattering (SANS) of solutions of glucose/xylose isomerase from *Streptomyces rubiginosus* was measured as a function of pressure. We show that the solution structure of the enzyme as seen by SANS is practically the same as in the crystal and is not changing with pressure up to 150 MPa. This reflects the unusually high structural stability of this material, which makes it extremely interesting to use also as secondary standard for pressure dependent SANS experiments. This lack of pressure dependence of the SANS data indicates also that any possible change in hydration of the protein induced by pressure is not visible in the SANS curves. A proper correction procedure must be used for the SANS data in order to account for the distortion of the intensity curve due to the hard sphere and electrostatic interactions. After this correction isomerase, the enzyme of a high conformational stability, can be readily used as a secondary standard for SANS measurements.

scattering standard; glucose/xylose isomerase; structure stability; Small Angle Neutron Scattering; high pressure; SANS

1. Introduction

Glucose/xylose isomerase from *Streptomyces rubiginosus* (D-xylose ketol-isomerase, EC 5.3.1.5.) is an intracellular enzyme of exceptional stability catalysing the isomerisation reaction of glucose and xylose. Four identical subunits of 43.3 kDa each, form a homotetramer. Each monomer is composed of two domains of which the larger one contains the $(\alpha/\beta)_8$ motif of the TIM (triose phosphate isomerase) barrel type.

The crystal structures of glucose/xylose isomerase from *Streptomyces rubiginosus*, deposited in PDB (Berman *et al.*, 2000), have already been solved by X-ray diffraction up to atomic resolution - 0.094 nm (PDB code: 2GLK; Katz *et al.*, 2006), 0.099 nm (PDB code: 1MNZ, Fig. 1) and also time-of-flight neutron diffraction with resolution 0.18 nm

(PDB code: 2GVE; Katz *et al*., 2006). Metal free enzyme and a number of complexes of this protein with the substrate analogues have been studied to the accuracy of 0.14-0.19 nm (Carrell *et al.*, 1989; Carrell *et al.*, 1994; Katz *et al.*, 2006).

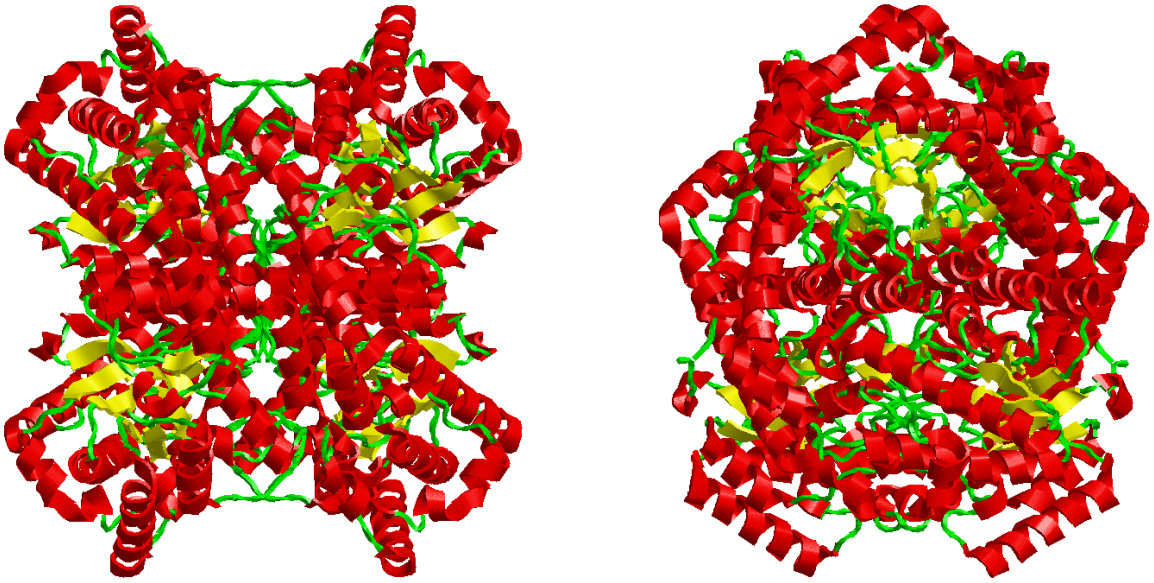

Figure 1 Structure of glucose/xylose isomerase from *Streptomyces rubiginosus* (D-xylose ketol-isomerase, EC 5.3.1.5) PDB code: 1MNZ. The model was rotated clockwise by 90° around the y-axis. The figure was prepared using the program RASTOP (Sayle & Milnerwhite, 1995).

This enzyme is one of the most widely used industrial enzymes and its activity is still on the same level even at temperatures of about 60°C (half-life of hundreds of days) (Visuri *et al.*, 1999).

Because of its high conformational stability on storage, thermal stability, radiostability during synchrotron radiation measurements, an appropriate molecular weight (173 kDa) and high reproducibility of the small angle X-ray scattering (SAXS) measurements, this enzyme has been proposed as a possible secondary standard of molecular weight in the SAXS measurements (Kozak, 2005).

The interfacial water molecules on the protein surface enter into specific type of interactions with the hydrophobic and hydrophilic amino acid residues forming a hydration shell whose physical properties differ significantly from those of bulk water. Correct recognition of the properties of this shell in different conditions determined by temperature, pressure and salt concentration are of key importance for explanation of the mechanism of protein folding, structure stability and protein-protein interactions. According to the small angle neutron scattering (SANS) and SAXS experimental results, water surrounding the protein surface can have a density by 15-20% greater than the bulk water (Svergun *et al.*, 1998). This phenomenon is, among others, a consequence of the electrostriction effect accompanying the strong electrostatic field around the charged residues (Merzel & Smith, 2002; Danielewicz-Ferchmin *et al.*, 2003; Merzel & Smith, 2005). Changes in the concentration of salt ions (Leberman & Soper, 1995),

pressure or temperature affect the properties of the hydration shell, disturb the water-protein interactions and destabilise the protein structure. The external hydrostatic pressure up to 300 MPa has no significant effect on the tertiary structure of the majority of proteins, however, as predicted by Danielewicz-Ferchmin *et al.* (2007) it should influence the density of water molecules in the range of the strong electrostatic fields on the protein surface. Assuming the structural stability in the pressure range 10-300 MPa, the changes in the hydration shell properties might be visible in the shape of the SANS and SAXS curves.

Although the hydrostatic pressure not exceeding 300 MPa has no significant effect on the tertiary structure of the majority of proteins, it can be sufficient for disturbing their quaternary structure (if they have it).

The effect of pressure on dissociation of oligomers has been widely documented in literature and concerns a wide range of particles: from dimers to multisubunit structures such as ribosomes or viruses (Silva *et al.*, 1996; Boonyaratanakornkit *et al.*, 2002). Dissociation of oligomers seems to be a universal phenomenon, although there are proteins that enhance their stability under elevated pressure. For instance, tetramer of glyceraldehyde-3-phosphate dehydrogenases (GAPDH) from thermophiles or hexamer of glutamate dehydrogenase (GDH) from the hyperthermophile *Pyrococcus furiosus* enhance their resistance to thermal inactivation under pressures up to 100 MPa (Hei&Clark,1994; Sun *et al.*,1999). Under pressure of similar, relatively low values, dissociation of dimers of lysozyme from hen egg white has been observed (Banachowicz, 2006). Tetramer of oxidase in the crystal state has been reported to begin to deteriorate close to 140 MPa (Colloc'h *et al.*, 2006). Tetramers of GAPDH from yeast, lactate dehydrogenase (LDH) form bovine and porcine, and malate dehydrogenase have been found to dissociate upon application of hydrostatic pressure up to 200 MPa (King&Weber, 1986; Ruan&Weber,1989)

The quaternary structure of isomerase seems stable even under pressures reaching 250 MPa (unpublished data).

Therefore**,** as our study is performed for pressures up to 150 MPa, it is reasonable to expect that the structure in solution as seen by SANS is practically the same as in the crystal. Furthermore, the structure of this protein has been shown to be unaffected by temperature (see above) and by variations in the ionic strength induced by increasing NaCl concentration. These observations reflect the unusually high degree of structural stability of this material, which makes it extremely interesting to use it also as a secondary standard for SANS experiments especially in the studies of protein conformation under elevated pressure. In order to correct for the relative changes in the protein scattering cross-section with pressure, requires taking into account the pressure dependence of the scattering length density of D_2O. The use of the so-called secondary scattering standards has been so far restricted to synthetic polymers. Unfortunately, these materials are characterised by size polydispersity. Thus any data evaluation is complicated. The proposed use of isomerase as the secondary standard permits avoiding the problems with the size polydispersity.

1.1. Sample Preparation

Glucose/xylose isomerase from *Streptomyces rubiginosus* was purchased from Hampton Research (USA). The buffer was exchanged and the enzyme was additionally purified by gel filtration. The protein solution (25mM TRIS

D_2O, 75mM NaCl, pH7.6) was concentrated by ultrafiltration using the Amicon Ultra-4 30k filters (Millipore). The protein concentration was determined by UV absorption at 280 nm ($A^{280}_{0.1\%}$=1.059) (Gill & Von Hippel, 1989).

1.2. SAXS Measurements

Synchrotron radiation scattering data were collected for the same sample at the EMBL SAS beamline X33 at the DORIS storage ring of the Deutsches Electronen Synchrotron (Hamburg, Germany) as previously described (Kozak, 2005). Samples of glucose isomerase with protein concentrations 3 and 6 mg/ml were used to eliminate concentration artefacts. The background data for the buffer were collected before and after data collection for the protein samples. The scattering of the buffer was subtracted and the final scattering curve was obtained by merging the scattering data collected at lower concentration with the data recorded at a higher concentration using the program PRIMUS (Konarev *et al.*, 2003).

1.3. SANS Measurements

The SANS experiments were performed at the SANS I instrument at the SINQ spallation source at the Paul Scherrer Institute (PSI) in Villigen, Switzerland (Kolbrecher & Wagner, 2000). Thermal neutrons of the wavelength λ = 0.5 nm with the wavelength spread $\Delta\lambda/\lambda$ of about 0.1 were used. Data analysis was made using the BerSANS software package (Keiderling, 2002), which accounts for all necessary corrections due to background, transmission, sample thickness, count rate/dead time ratio, masking and radial averaging of the raw data. A standard water sample (for discussion of the details of absolute calibration see chapter 2.1.) was used for calibration to absolute scattering intensities and also to account for non-uniform detector efficiency (Strunz *et al.*, 2000). The applied calibration procedure also included the correction for inelastic and multiple scattering contributions necessary if water is used as a secondary standard by correcting the water cross section with a wavelength dependent term $g(\lambda)$, which at the SANS instrument used is practically identical to the one of the SANS instrument D22 at ILL published by Lindner (Lindner, 2000). The $g(\lambda)$ dependence was obtained during commissioning of SANS-1 at PSI by comparing the incoherent scattering of H_2O with the forward scattering of a polystyrene sample of very narrow molecular weight distribution. After this correction and the calibration procedures, the scattering cross-sections $\frac{d\Sigma_S}{d\Omega}(q)$ in [cm^{-1}] were obtained and used throughout the paper. As an input to the CRYSON program the primary beam profile was measured and was used to account for smearing effects. The measurements were performed at two different detector positions at 2 and 6 meters distance from the sample, which gave access to a q-range of $0.02 < q < 3.5$ nm^{-1}, where q is the scattering vector, defined as $q = |\mathbf{q}| = \frac{4\pi}{\lambda}\sin\frac{\theta}{2}$, with λ being the neutron wavelength and θ being the scattering angle.

1.4. Pressure Cell

A custom made high pressure cell was used, which allows measurements of liquid samples at pressures up to 500 MPa and temperatures from 5 to 50°C (Kolbrecher *et al.*, 2007). Care was taken to separate the sample of approximately 1 mm thickness from the oil transmitting hydrostatic pressure, generated by a Nova-Swiss moving piston hand pump. The pressure cell was equipped with large sapphire windows to withstand the pressure. The transmission of the cell is about 0.6 for λ = 0.5 nm and causes no considerable excess scattering in the q-range used.

2. Analysis of the SANS data

2.1. Absolute calibration: The problem

The use of various scattering standards has been reported for SANS measurements. Among them, the use of light water samples is most frequently chosen. A rather extensive discussion on that issue has been given by Wignall & Bates (1987). In general the calibration standards can be divided in two groups: the so called incoherent scatteres, like water, Lupolen (which is partly crystalline PE), PMMA or vanadium, and the coherently scattering standard samples, like polymers in solution. If the molecular weight of the polymers has been established by other methods, then from the measurement of the forward scattering a calibration can be obtained. Porous samples with calibrated internal surface can be also used. A special way is the so-called direct beam method. All these methods have specific advantages and drawbacks. For incoherent scatterers, the error in values of the absolute intensity is about 2% according to Jacrot & Zaccai (1981). Primary standards suffer from the fact that they scatter little, moreover inelastic effects in water as discussed by Gosh & Rennie (1990) and deviations from isotropic scattering in case of Lupolen due to crystallinity have to be taken into account.

Another attempt is to use the so-called secondary standards. Lindner (2000) has discussed the use of secondary standards such as narrowly distributed poly(styrene) PS samples (characterised by stronger scattering) for verification of the water calibration. The scattering from a polymeric standard with a molecular weight of about 40 kDa at low q is easily one order of magnitude higher than scattering from primary standards. Scattering can be increased of course, if higher molecular weights are used. Among the coherently scattering secondary standards the use of polymeric materials suffers especially from their polydispersity and hence from the preparation conditions, which in turn renders the reproducibility complicated. Moreover, next to the molecular weight distribution also the molecular volume of the polymer in solution and not the molecular volume of the bulk polymer, has to be known. In principle this can be obtained by a precise pycnometric (or density) measurement. Here the use of biological molecules is favoured, since they are monodisperse and their structure and volume do not change upon solvation in water. This is a reasonable assumption as the protein is a globular and compact object in contrast to polymers in solution. In this paper we want to propose the use glucose isomerase as a secondary scattering standard, which is by its nature monodisperse, can be easily obtained by standard preparation procedures and its solutions are stable against large ranges of temperature, pressure and ionic strength. Its molecular weight of about 173 kDa and thus its size assures

that the plateau of the scattering curve is reached at q-values smaller than 0.2 nm^{-1}, which allows a reliable determination of the forward scattering. The q-value of 0.2 nm^{-1} is well accessible by all SANS machines.

2.2. The data evaluation of isomerase

The raw SANS data were analysed in the usual way using the BerSANS software package, as already outlined in chapter 1.3.

The scattering cross section $\frac{d\Sigma_S}{d\Omega}(q)$ in cm^{-1} is related to the physical properties of the protein in solution via:

$$I_S(q)K_N = \frac{d\Sigma_S}{d\Omega}(q) = \frac{N}{V_{tot}}(b - V\rho_0)^2 P(q)S(q) = c\frac{N_A}{M_W}(b - V\rho_0)^2 P(q)S(q) \qquad (1)$$

where b is the scattering amplitude (scattering length) of isomerase, V its volume and ρ_0 is scattering length density of the solvent, N is the number of particles in the illuminated volume and $c = \frac{NM_W}{V_{tot}N_A}$ is the particle concentration in g/cm^3 with V_{tot} being the illuminated sample volume, N_A the Avogadro number and M_W the molecular weight. $P(q)$ is the form factor, which is normalized to 1 for q=0 and $S(q)$ is the structural factor, which takes into account the inter-particle correlations. The constant K_N depends on experimental details. $I_S(q)$ is the experimentally measured scattering curve in arbitrary units and has to be multiplied by the constant K_N, which includes all instrumental parameters (Wignall & Bates, 1987), to convert it in absolute units of cm^{-1}. As we are interested in the determination of $\frac{d\Sigma_S}{d\Omega}(q)$ for q=0, we have to take into account that $S(q$=0) can take values considerably lower than 1, depending on the ionic strength, concentration and charge. Consequently, we have to take these effects into account in determination of $\frac{d\Sigma_S}{d\Omega}(q=0)$. In order to proceed we have divided the data treatment procedure according to Eq. (1) in three steps:

i) determination of the form factor $P(q)$ for isomerase from the crystallographic data,

ii) evaluation of the structural factor $S(q)$ of isomerase solutions, and finally

iii) calculation of the scattering cross section $\frac{d\Sigma_S^{corr}}{d\Omega}(q=0)$ corrected for the structure factor as well as the estimation of the protein volume V.

3. Results and Discussion

3.1. The form factor *P(q)*

A comparison of the experimental scattering curves $I_S(q)$ measured by means of SANS (concentration of 22.7 mg/cm^3) and SAXS (concentration of 3 and 6 mg/ cm^3) is shown in Fig. 2.

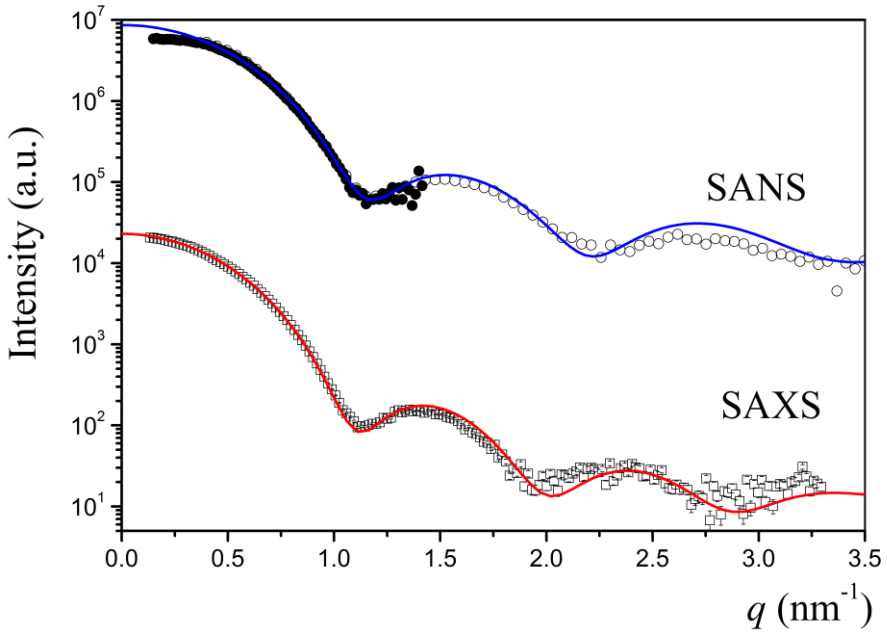

Figure 2 SANS: isomerase concentration 22.7 mg/ cm^3 (25mM TRIS in D_2O, 75mM NaCl, pH7.6), solid circle for sample-detector distance 6 m and open circle for 2 m; SAXS: open square, the same salt as before [M. Kozak, J. Appl. Cryst. **38**, 555 (2005)]; solid lines are the results of CRYSON and CRYSOL simulation for SANS and SAXS respectively, based on crystal structure. SANS curve is below CRYSON for low q due to influence of $S(q)$. Curves are shifted vertically for clarity.

The fit of SAXS data and crystal structure (PDB code: 1MNZ) was obtained for $\delta\rho$ = 10 e/nm^3, while the fit of SANS data and crystal structure was obtained for the contrast of the solvation shell 0.4314, D_2O fraction in solvent 0.7. As one can see in this figure, all important features of the shape of these curves are practically identical, although the neutron beam is by a few orders of magnitude less monochromatic ($\Delta\lambda/\lambda$=0.1) than the X-ray beam from the synchrotron. Both curves are shifted vertically in order to compare the two methods only and are therefore not presented in absolute scales. The lack of sharp minima in the calculated curves results from a non-spherical shape of the protein, however, the ellipticity is only of a few percent. Small deviations from spherical shape result in strongly smeared out minima. For spheres with a shape variance of 2% such an effect can already be observed. Different positions of the higher minima and maxima in SAXS and SANS experimental curves are in agreement with the curves calculated for the same crystal structure of isomerase using CRYSOL (Svergun *et al.*, 1995) and CRYSON (Svergun *et al.*, 1998), respectively. In this way a reliable determination of the form factor of the protein is made and its value will be used in further calculations. The SANS data (symbols) deviate from the calculated form factor (solid line) in the low q-range because at higher concentrations the structural factor is substantially different from 1. As the concentration of the protein in the SAXS experiment was lower by almost one order of magnitude compared to the SANS experiment, both experimental and calculated curves are identical, indicating $S(q)$=1. This effect is discussed in detail in the next chapter.

Both SANS and SAXS curves deviate slightly at high q from the lines simulated for the crystal isomerase structure using CRYSON and CRYSOL, respectively. This deviation might be due to the fact that the hydration water shell has not been taken into account properly. In the CRYSON program a hydration shell of a uniform thickness and density all over the protein surface is assumed. Theoretical studies (Merzel & Smith, 2005; Danielewicz-Ferchmin *et al.*, 2006) however indicate that the hydration of proteins is not uniform: charged hydrophilic regions of the protein surface are strongly hydrated, while the hydration layer on the hydrophobic regions might be much thinner or non-existing.

3.2. The determination of *S*(*q*)

The scattering curves obtained for isomerase solutions at concentrations of 4.54 and 22.7 mg/ cm^3 at ambient pressure and temperature of 20ºC are shown in Fig. 3 (symbols). In this figure the $P(q)$ curve calculated for the crystal structure (PDB code: 1MNZ) by means of the CRYSON program is shown as a solid line. A reasonable agreement between the calculated and measured curves can be seen for the low concentration solution, indicating that the solution structure of the isomerase is very close to that in the crystal. In high concentrations a strong systematic deviation of the calculated curve from the experimental one can be seen at the low q-range. A similar but much smaller deviation is also seen for the low concentration curve.

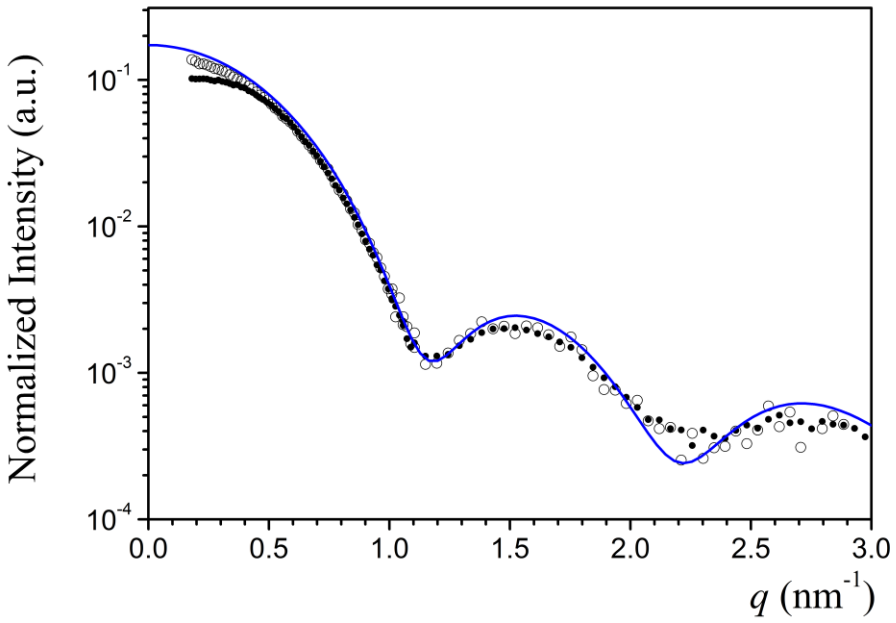

Figure 3 Experimental intensities $I(q)$ normalized with concentration for isomerase concentrations of 4.54 (open symbols) and 22.7 mg/ cm^3 (solid symbols), (25 mM TRIS in D_2O, 75mM NaCl, pH7.6). The solid line is generated by CRYSON for the crystal structure of the isomerase. Experimental intensities are smaller than the CRYSON result at low q due to the influence of $S(q)$.

The deviations of the experimental intensity curve measured at high concentration from that measured at low concentration and calculated using CRYSON program and the crystal structure, seen in Fig. 3 at low *q*'s, can be explained as follows:

The scattered intensity for a protein solution (Eq. 1) depends on the form factor *P*(*q*), which depends on the size and shape of the protein, and the structure factor *S*(*q*), which describes the radial distribution (radial ordering) of the proteins in solution in the following way: $I(q) \propto P(q)S(q)$. In the case of non interacting dilute protein solutions, the structure factor *S*(*q*)=1 for all *q*'s, *I*(*q*) $\propto$ *P*(*q*). If, however, the proteins are interacting through long-range electrostatic interactions resulting from incomplete screening of the protein charges, *S*(*q*)≠1 and *I*(*q*) is not proportional to *P*(*q*) only, but *S*(*q*) must be also included. The effect of electrostatic interactions on *S*(*q*) can be estimated using the rescaled mean-spherical approximation RMSA (Nägele, 1996). The *S*(*q*), *P*(*q*) and *I*(*q*) curves calculated using the RMSA model for the radius of the protein *R*=3.8 nm and a charge of about 5.6076×10^{-18} C (35 elementary charges) at the salt concentration of 75 mM are shown in Fig.4.

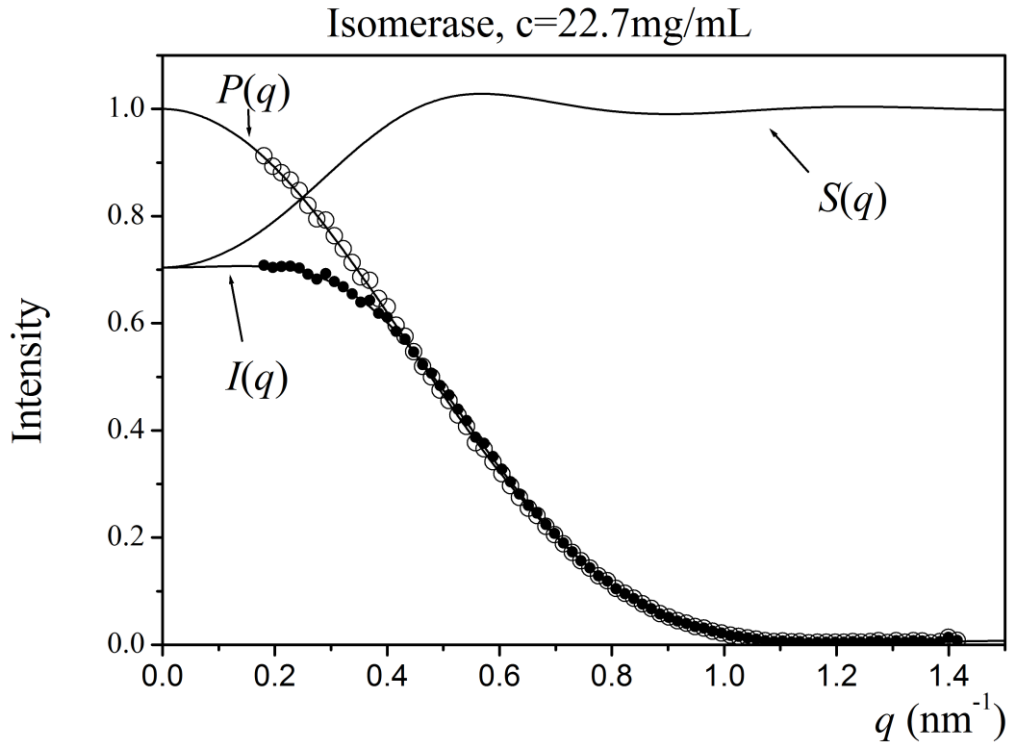

Figure 4 The *P*(*q*), *S*(*q*) and *I*(*q*) curves calculated for a sphere using the RMSA model with the parameters: *R*=3.8 nm, c=22.7 mg/ cm^3, charge/protein=5.6076×10^{-18} C (35 elementary charges), NaCl concentration 75 mM. Not corrected (•) and corrected (o) experimental data measured at a concentration of 22.7 mg/ cm^3 are also shown. The corrected data is well fitted by the form factor *P*(q).

As one can see, the theoretical *I*(*q*) curve coincides nicely with the experimental data and the deviation of the experimental *I*(*q*) from the theoretical *P*(*q*) curve calculated from the protein structure is quantitatively explained and is due to the long-range interactions and the resulting *S*(*q*). It means that at the concentrations of isomerase used in

this experiment, the salt concentration of 75 mM is insufficient to screen the long-range electrostatic interactions. It also means, that the part of the $I(q)$ curve which deviates from $P(q)$ in the low q-range should be used neither for the fit using the CRYSON program nor for the Guinier plot.

The $S(q)$ correction depends on the protein charge and concentration as well as the salt concentration and can be calculated using the RMSA model. In order to illustrate this effect we have plotted S (q=0) versus isomerase concentration for different salt concentrations in the range from 1 to 500 mM and compared it with the curve calculated for the hard sphere model, Fig. 5. The same data are plotted versus the salt concentration for the protein concentrations in the range of 1 – 100 mg/cm^3, Fig. 6. In these calculations, the protein charge was fixed to 5.6076×10^{-18} C (35 elementary charges).

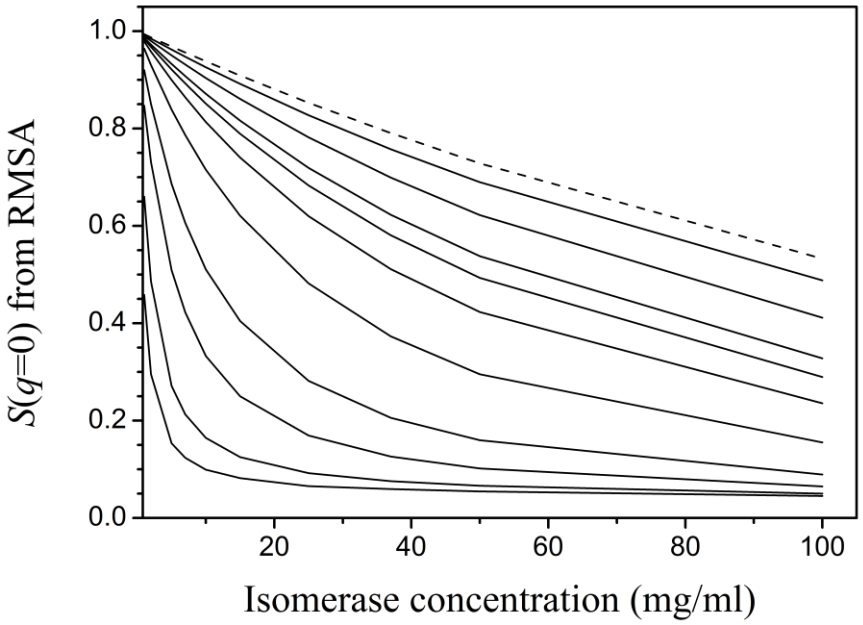

Figure 5 The dependence of the value of $S(q=0)$, calculated using the RMSA model, on the isomerase concentration for salt concentrations in the range of 1-500 mM, compared with data for hard sphere. Solid lines from bottom to top: salt concentration 500, 200, 100, 75, 50, 25, 10, 5, 1 mM; dashed line: hard sphere.

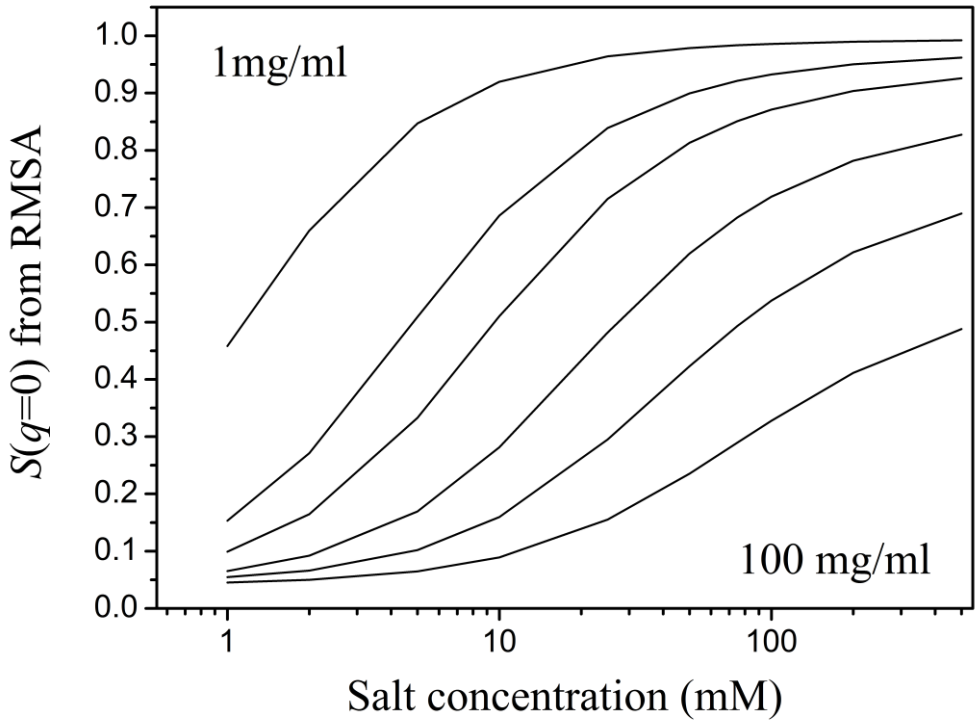

Figure 6 The dependence of the value of $S(q=0)$, calculated using the RMSA model, on salt concentration for isomerase concentrations in the range of 1-100 mg/cm^3 and protein charge 5.6076×10^{-18} C (35 elementary charges). Solid lines from top to bottom:1, 5, 10, 25, 50, 100 mg/cm^3, as indicated in the figure.

Another approach taking into account the concentration effects is based on the analysis of the forward scattering. The value for $S(q=0)$ is related to the osmotic pressure Π of the particle solution,

$$S(q=0)=\frac{RT}{M_W}\left(\frac{\partial\Pi}{\partial c}\right)^{-1} \qquad (2)$$

where R is the gas constant and T the absolute temperature. We can expand the derivative to get:

$$\frac{\Pi}{cRT}=\frac{1}{M_W}+A_2\,c+.... \qquad (3)$$

where A_2 is the 2nd virial coefficient, which depends on the interaction pair potential between particles in solution. Usually, A_2 is obtained from the slope of the linear fit:

$$\frac{1}{S(c,q=0)}=1+2M_W A_2 c+... \qquad (4)$$

In Fig. 7 we plot the reduced quantity $\frac{1}{c}\left(\frac{1}{S(c,q=0)}-1\right)=2M_W A_2$ versus the salt concentration.

Clearly for the protein concentrations lower than 5 mg/cm^3 all so reduced structure factors coincide thus indicating that for these low concentrations the structure factor is well described by Eq. (4) and A_2 is only dependent on the salt concentration but becomes independent of the isomerase concentration.

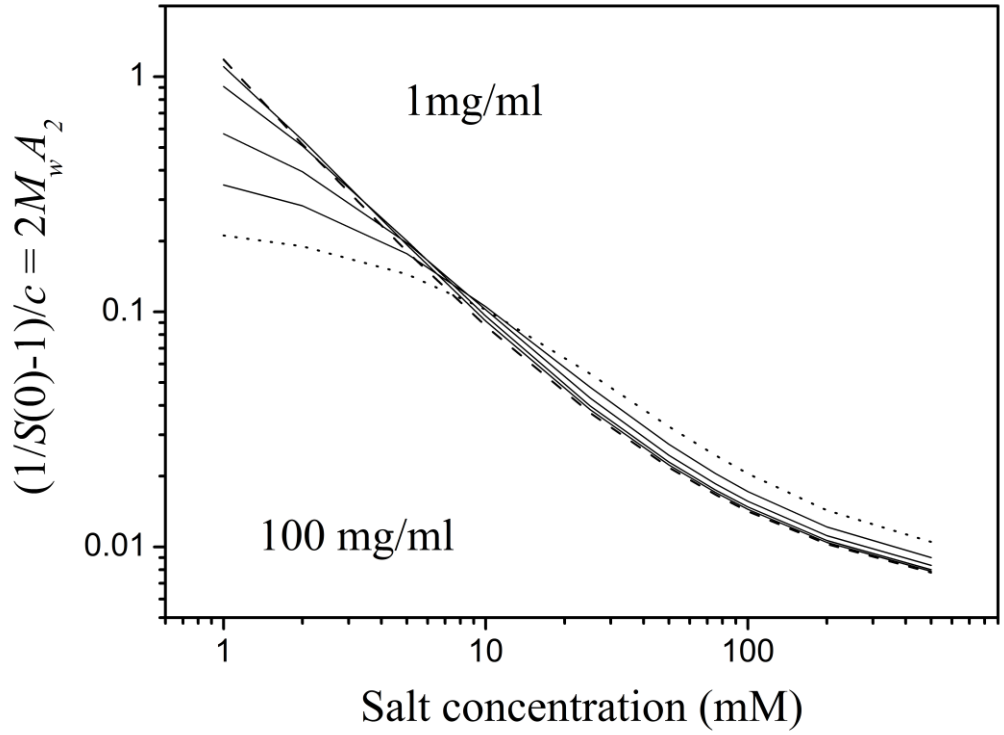

Figure 7 The dependence of the reduced value of $\frac{1}{c}\left(\frac{1}{S(c,q=0)}-1\right)$, on salt concentration for isomerase concentrations in the range of 1-100 mg/cm^3, dashed line: 1 mg/cm^3; solid lines: 5, 10, 25 and 50 mg/cm^3; dotted line: 100 mg/cm^3 as indicated in the figure.

3.3. Determination of the correct $I_s(q=0)$ and the protein volume V

From the experimentally measured $I_s(q)$ curves one can obtain the value of $\frac{d\Sigma_S^{\exp}}{d\Omega}(q=0)$, rewriting Eq. (1) for $q=0$ as:

$$\frac{d\Sigma_S}{d\Omega}(q=0)=c\frac{N_A}{M_w}\left(\frac{b}{V}-\rho_0\right)^2 V^2 S(q=0)=c\frac{N_A}{M_w}(b-\rho_0 V)^2 S(q=0)=I_S(q=0)K_N \qquad (5)$$

where $\Delta\rho=\frac{b}{V}-\rho_0$ is the scattering contrast of the protein, b is the scattering length, V – the volume and b/V – the scattering length density of the protein and ρ_0 is the scattering length density of the solvent. Note that the

formulation of Eq. (5) with $\Delta\rho$ implies that we have two volume dependent terms on the rhs of the equation, whereas the use of $(b-\rho_0 V)^2$ permits avoiding that problem and makes the determination of V unambiguous. The length b can be obtained from the atomic composition of the protein using CRYSON or other programs. Thus, in order to obtain the protein volume V we have to know the value of $S(q=0)$, which depends on the salt and the protein concentrations, as discussed earlier. For spherical particles the values of $S(q)$ and in particular $S(q=0)$ can be calculated using the RMSA model and are given in Figs. 5 and 6 for different protein and salt concentrations. The value of the corrected scattering cross-section can be then calculated using the values of the $S(q=0)$ obtained from RMSA: $\frac{d\Sigma_S^{corr}}{d\Omega}(q=0) = \frac{d\sum_S^{\exp}}{d\Omega}(q=0) \Big/ S(q=0)$

The values of $S(q=0)$, the scattering cross-sections $\frac{d\Sigma_S^{\exp}}{d\Omega}(q=0)$ and $\frac{d\Sigma_S^{corr}}{d\Omega}(q=0)$ and the corresponding volumes, calculated using Eq. (5) are given in Table I.

Table 1 The values of the experimentally measured scattering cross-sections $\frac{d\Sigma_S^{\exp}}{d\Omega}(q=0)$ and the corrected scattering cross-sections $\frac{d\Sigma_S^{corr}}{d\Omega}(q=0)$ obtained using RMSA as well as the corresponding values of the molecular volume V and V_{corr} calculated using Eq. (5) and the values of $S(q=0)$ obtained from RMSA.

	Not corrected		RMSA correction		
c	$\frac{d\Sigma_S^{\exp}}{d\Omega}(q=0)$	V	S(q=0)	$\frac{d\Sigma_S^{corr}}{d\Omega}(q=0)$	V_{corr}
(mg/ml)	(cm^{-1})	(nm^3)		(cm^{-1})	(nm^3)
22.7	2.311	190	0.704	3.2827	206
4.54	0.628	204	0.928	0.6767	207
2.27	0.333	207	0.963	0.3457	209

As follows from Table I, the use of the experimental (not corrected) values of $\frac{d\Sigma_S^{\exp}}{d\Omega}(q=0)$ results in too low values of the protein volume, which, additionally, depend on the protein concentration. When the corrected values of $\frac{d\Sigma_S^{corr}}{d\Omega}(q=0)$ are used, the correct, almost constant values of the volume are obtained.

We can furthermore take advantage from the fact that the measurements were performed at different protein concentrations. This will lead to an increase in statistical accuracy compared to that obtained with only one dataset.

In order to do so, a convenient way to analyse the intensity data in terms of Eq. (7) is to plot $\frac{d\Sigma_S^{corr}}{d\Omega}(q=0)$ versus the protein concentration *c*, Fig. 8. The slope of this line, for *c* expressed in [mg/cm^3] is:

$$\frac{\frac{d\Sigma_S^{corr}}{d\Omega}(q=0)}{c} = \frac{N_A}{M_w}(b-\rho_0 V)^2 \qquad (6)$$

and does not depend on the protein concentration (straight line). It allows a reliable determination of the protein volume.

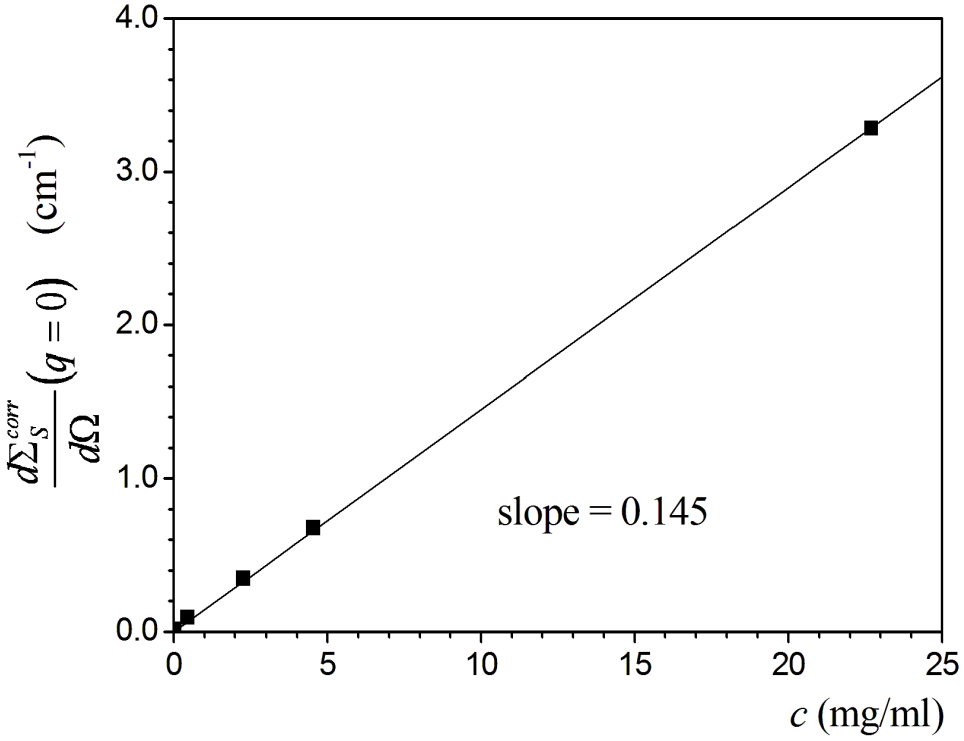

Figure 8 Absolute scattered intensity extrapolated to *q*=0 $\frac{d\Sigma_S^{corr}}{d\Omega}(q=0)$ plotted versus protein concentration.

The scattering length of the protein estimated using CRYSON amounts to $b=6.73\times10^{-9}$ cm, the scattering length density of the solvent to $\rho_0=6.40\times10^{10}$ cm^{-2} and the molecular weight of the protein M_w=173200 D. The only adjustable parameter in Eq. (6) is the protein volume *V*. Using the experimentally obtained slope, standard water calibration (Fig. 8) of 0.145 cm^2/mg and the protein parameters listed above, we obtain the protein volume *V*=206 nm^3, thus the scattering length density $b/V=3.27\times10^{10}$ cm^{-2} and the contrast $\Delta\rho=b/V-\rho_0=-3.13\times10^{10}$ cm^{-2}. This experimentally obtained protein volume is in a good agreement with the dry protein volume calculated from the crystal structure using CRYSON, which amounts to 211 nm^3. Such a good agreement of the value of the protein volume within ±2% obtained from our SANS data using water calibration with the dry volume of crystal structure

indicates that the overall isomerase structures in solution and in crystal are very similar (or identical). Additionally, it confirms the correctness of our data correction procedures and the water calibration.

3.4. Absolute calibration of the scattering cross-section of a sample

Using Eqs. (1) and (6) we have:

$$slope(R) = \frac{\frac{d\Sigma_R^{corr}}{d\Omega}(q=0)}{c_R} = \frac{\frac{d\Sigma_R^{\exp}}{d\Omega}(q=0)/S_R(q=0)}{c_R} = \frac{I_R^{\exp}(q=0)}{S_R(q=0)c_R}K_N \qquad (7)$$

where the lhs of Eq. (7) is the slope of the line in Fig. 8, which for isomerase amounts to *slope(R)*=0.145 cm^2/mg. The subscript "*R*" stands for the reference, i.e. isomerase. Thus, the calibration constant K_N can be calculated as

$$K_N = \frac{0.145 S_R(q=0)c_R}{I_R^{\exp}(q=0)} \qquad (8)$$

Using this calibration constant, the absolute scattering cross-section (in cm^{-1}) of a new sample (S) can be easily calculated.

4. Isomerase under compression

In order to check whether isomerase can be a good standard sample also in pressure dependent studies, the pressure dependence of $I(q)$ at the concentration of 2.54 mg/cm^3 and at the constant temperature of 20^{o}C, was measured in the pressure range from 1 to 150 MPa using SANS and is shown in Fig. 9. The raw curves showed a systematic increase in the intensity with increasing pressure. This observation can be explained by the fact that the increase in the scattering length density of the solvent due to the compression of the solution is to a good approximation given by the pressure induced change in the density of heavy water, which amounts to 4.3% change per 100 MPa. As can be seen from Eq. (5) this effect enters quadratically in the expression of the contrast and is thus important. We find from our experimental data that the increase in the forward scattering amounts to 17% per 100 MPa. On the other hand, using the 4.3% density change per 100 MPa the contrast variation with pressure was calculated to be of about 18% per 100 MPa, which accounts quantitatively for the observed effect. For clarity we have superimposed these curves in order to find out whether a change in the shape occurs under the action of pressure, see Fig.9.

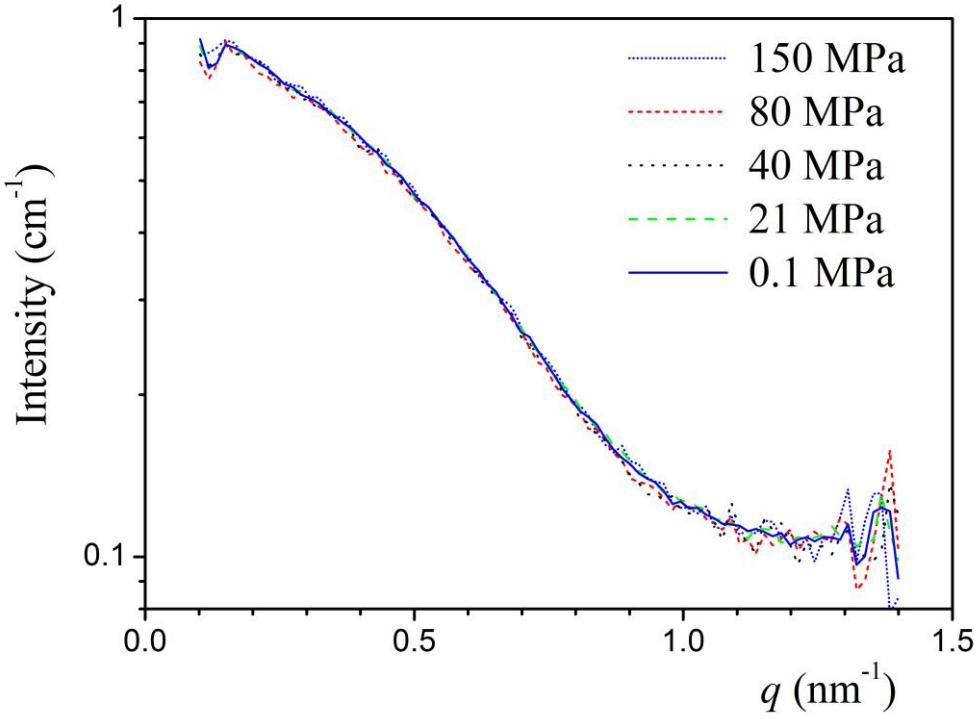

Figure 9 (Colour online) Experimental I(q) curves measured for the isomerase solution of concentration of 2.54 mg/ml at 20ºC (25mM TRIS in D_2O, 75mM NaCl, pH7.6) for pressures indicated in the Figure.

The $I(q)$ curves at all pressures collapse on a master curve and indicate no dissociation or conformational change of isomerase in this pressure range. This finding also supports our previous assumption that the increase in the forward scattering intensity is only due to the pressure induced change in the scattering length density of water and is not related to changes in the protein structure which would give rise to a different b/V value. With regard to the structure we have thus to conclude that obviously the structure of the isomerase in solution is very dense, as was already speculated fitting the $P(q)$ with CRYSON leading to structural parameters very close to those obtained for the conformation in the crystal. It means that the structure does not contain any loose or markedly less dense regions, which in turn would act as targets for pressure. Glucose isomerase was found to be conformationally stable up to 150 MPa and thus offers the possibility to be used as a scattering standard even under conditions of high pressure. Furthermore, it is well known that also other biological molecules exhibit no change in structure even at higher pressures due to the stabilizing effect of electrostatic interactions in combination with hydrogen bonding. Changes in structure are typically observed for P>500 MPa for a number of monomeric biopolymers. In a preliminary test we have found no changes in the scattering curve for egg white lysozyme up to 350 MPa. Likewise bovine serum albumin was found to be stable up to 450 MPa. A secondary standard, besides a high pressure stability, must also exhibit the following features: high monodispersity, no aggregation, well characterized crystallographic structure and nearly spherical shape, so the $S(q)$ can be calculated using RMSA model. All these conditions are fulfilled by isomerase. Therefore, we propose isomerase to be used as a secondary scattering standard.

Practically identical shape of the scattering curves $I(q)$ obtained for isomerase for all pressures also indicates, that not only the protein structure is insensitive to pressure in this pressure range but also there are no visible changes in hydration that can be detected by SANS. This finding further supports the idea of using this protein as a secondary standard in the SANS experiments.

5. Conclusions

Pressure dependence of the small angle neutron scattering (SANS) was measured for solutions of glucose/xylose isomerase from *Streptomyces rubiginosus* of different concentrations in the pressure range of 0.1-150 MPa. It was found that the experimental form factor of the protein was practically identical to that calculated using the crystallographic structure and did not change with pressure. This indicates that the solution structure of the enzyme is the same as that in the crystal and does not depend on pressure in the pressure range studied. Additionally, no changes in hydration with pressure were detected for this protein using SANS.

The deviation of the intensity curve $I(q)$ from the form factor $P(q)$ in the low q-range is quantitatively explained using the RMSA model as resulting from the structure factor $S(q)\neq 1$, due to the hard-sphere and electrostatic interactions.

The extrapolated to $q=0$ scattered intensity corrected for the $S(q)\neq 1$ can be used to calculate the protein volume and results in practically concentration independent volume values which are in agreement with the volume calculated for the crystalline protein structure. We find no indication for aggregation behaviour in the entire concentration range studied.

Taking into regard its very high structural stability the glucose/xylose isomerase from *Streptomyces rubiginosus* can be used as a secondary standard in pressure dependent SANS experiments

Acknowledgements Partial financial support of the EU NoE SoftComp project is gratefully acknowledged. This work is based on experiments performed at the Swiss spallation neutron source SINQ, Paul Scherrer Institute, Villigen, Switzerland. We especially are indebted to Dr. Ralf Biehl for helpful discussions.

References

Banachowicz, E. (2006) *Biochim. Biophys. Acta* ,**1764**, 405-413.

Berman, H. M., Westbrook, J., Feng, Z., Gilliland, G., Bhat, T. N., Weissig, H., Shindyalov, I. N. & Bourne, P.E. (2000). *Nucleic Acids Research*, **28**, 235-242.

Boonyaratanakornkit, B.B., Park, C.B.& Clark, D.S.,(2002). *Biochim. Biophys. Acta* **1595**, 235–249.

Carrell, H. L., Glusker, J. P., Burger, V., Manfre, F., Tritsch, D. & Biellmann, J. F. (1989). *Proc. Natl.Acad. Sci.* **86**, 4440-4444.

Carrell, H. L., Hoier, H. & Glusker, J. P. (1994). *Acta Cryst. D***, 50**, 113-123.

Colloc'h, N., Girard, E., Dhaussy, A.C., Kahn, R., Ascone, I., Mezouar, M. & Fourme, R. (2006) *Biochim Biophys Acta*.**1764(3)**,391-397.

Danielewicz-Ferchmin, I., Banachowicz, E. &Ferchmin, A.R.(2003) *Biophys Chem.* **106(2)**, 147-153.

Danielewicz-Ferchmin, I., Banachowicz, E. &Ferchmin, A.R. (2006) *Chem.Phys.Chem*. **7(10)**, 2126-2133 .

Danielewicz-Ferchmin, I., Banachowicz, E. &Ferchmin, A.R. (2007) *J. Mol. Liquids* **135(1-3)**, 75-85.

Gill, S. C. & Von Hippel, P. H. (1989). *Anal. Biochem.* **182**, 319-326.

Gosh, R. E. & Rennie, A. R. (1990). *Inst. Phys. Conf. Ser.* **107**, 233-244.

Hei, D.J. & Clark, D.S.,(1994) *Appl. Environ. Microbiol*.**60(3)**,932-939.

Jacrot, B. & Zaccai, G. (1981) *Biopolymers*, **20**, 2413-2426.

Katz, A.K., Li, X., Carrell, H.L., Hanson, B.L., Langan, P., Coates, L., Schoenborn, B.P., Glusker, J.P., Bunick, G.J. (2006) *Proc. Natl. Acad. Sci. USA* **103**, 8342-8347.

Keiderling, U. (2002) *Appl. Phys. A*, **74**, S1455–S1457.

King, L. & Weber, G. (1986) *Biochemistry* **25(12)**,3632-3637

Kohlbrecher, J. & Wagner, W. (2000). *J. Appl. Cryst.* **33**, 804-806.
Kohlbrecher, J., Bollhalder, A., Vavrin, R. &. Meier, G.(2007). *Rev. Sci. Instrum*., **78**, art. no. 125101.

Konarev, P. V., Volkov, V. V., Sokolova, A. V., Koch, M. H. J. & Svergun, D. I., (2003). *J. Appl. Cryst.* **36**, 1277-1282.

Kozak M. (2005). *J. Appl. Cryst.* **38**, 555-558.

Leberman, R.& Soper, A. K. (1995) *Nature* **387**, 364-366 .

Lindner, P. (2000). *J. Appl Cryst.* **33**,807-811.

Merzel, F. & Smith, J.C.(2002). *Proc. Natl. Acad. Sci.* USA. **99(8)**, 5378-5383 .

Merzel, F. & Smith,J.C. (2005) *J. Chem. Inf. Model*. **45(6)**, 1593-1599 .

Nägele, G. (1996). *Phys. Rep.* **272**, 215-372.

Ruan, K. & Weber, G. (1989) *Biochemistry*. **28(5)**, 2144-2153.

Sayle, R. A. & Milnerwhite, E. J. (1995) *Trends Biochem. Sci*. **20**, 374–376.

Silva, J.L., Foguel, D., Da Poian, A.T. & Prevelige, P.E.,(1996). Curr. Opin. Struct. Biol. 6(2), 166-175.

Sun, M.M., Tolliday, N., Vetriani, C., Robb, F.T. & Clark, D.S. (1999). Protein Sci. 8(5),1056-1063.
Strunz, P. Saroun, J., Keiderling, U., Wiedenmann, A. & Przenioslo, R. (2000). *J. Appl. Cryst.* **33**, 829-833.
Svergun, D. I., Barberato, C. & Koch, M. H. J. (1995). *J. Appl. Cryst.* **28**, 768-773.

Svergun, D. I., Richard, S., Koch, M. H .J., Sayers, Z., Kuprin, S. & Zaccai, G. (1998). *Proc. Natl.*

Acad. Sci. **95**, 2267-2272.

Visuri, K., Pastinen, O., Wu, X. Y., Makinen, K. & Leisola, M. (1999). *Biotechnol. Bioeng.* **64**, 377-380.

Wignall, G. D. & Bates, F. S. (1987). *J. Appl Cryst.* **20**, 28-40.